Investigations of excitation energy transfer and intramolecular interactions in a nitrogen corded distrylbenzene dendrimer system

O. Varnavski
Department of Chemistry, Wayne State University, Detroit, Michigan 48202

I. D. W. Samuel
Ultrafast Photonics Collaboration, School of Physics and Astronomy, University of St. Andrews, North Haugh, St. Andrews, KY16 9SS, United Kingdom

L.-O. Pålsson
Department of Physics, University of Durham, South Road, Durham DH1 3LE, United Kingdom

R. Beavington and P. L. Burn
Dyson Perrins Laboratory, South Parks Road, Oxford, OX1 3QY, United Kingdom

T. Goodson III[a)]
Department of Chemistry, Wayne State University, Detroit, Michigan 48202

(Received 1 October 2001; accepted 27 February 2002)

The photophysics of an amino-styrylbenzene dendrimer (A-DSB) system is probed by time-resolved and steady state luminescence spectroscopy. For two different generations of this dendrimer, steady state absorption, emission, and photoluminescence excitation spectra are reported and show that the efficiency of energy transfer from the dendrons to the core is very close to 100%. Ultrafast time-resolved fluorescence measurements at a range of excitation and detection wavelengths suggest rapid (and hence efficient) energy transfer from the dendron to the core. Ultrafast fluorescence anisotropy decay for different dendrimer generations is described in order to probe the energy migration processes. A femtosecond time-scale fluorescence depolarization was observed with the zero and second generation dendrimers. Energy transfer process from the dendrons to the core can be described by a Förster mechanism (hopping dynamics) while the interbranch interaction in A-DSB core was found to be very strong indicating the crossover to exciton dynamics. © *2002 American Institute of Physics.* [DOI: 10.1063/1.1471241]

I. INTRODUCTION

The control of energy transfer in macromolecular architectures such as organic polymers, chromophore assemblies, and dendrimers is a major goal toward possible applications in light harvesting. Organic dendrimers[1] have shown great promise for energy funneling processes as well as several other possible applications including light emitting diodes,[2–5] solid-state organic laser devices,[6] new nanocomposite materials[7] and artificial light-harvesting systems.[8] These applications, and the fundamental physics and chemistry behind novel dendritic macromolecular architectures, have motivated the investigation of the mechanisms involved in the energy transfer processes in novel organic dendrimers.[7–12] There has been a widespread interest in the research to mimic the natural photosynthesis process. Natural photosynthetic systems have been investigated for their light harvesting properties by a variety of methods. Several research groups have contributed to the vast amount of information known about particular natural light harvesting systems that have been shown to harvest absorbed light over nanometer distances with very high efficiencies.[13–16] Organic dendrimers are a keen artificial architectural choice for directed energy transduction due to their well-defined structures and synthetic ease. Linear chain polymers are limited in this regard due to their flexibility and strong interchain interactions.[17] These interactions may result in a strong fluorescence quenching at defect sites as well as in the formation of excimers, which may trap the energy at a particular site, interrupting the energy transfer process to the core.

Artificial light harvesting systems such as dendrimers have already shown (in part) similar qualities as their photosynthetic counterparts.[6,17–22] Critical works by Aida,[19,21] Moore,[20,22] and Frechet[6] have provided the synthetic basis for the development of useful dendritic architectures for efficient energy transfer. Aida's dendrimer system (a poly-(aryl)ether) harvests low-energy photons and transfers the energy to an azobenzene core.[21] Moore's system is based on phenylacetylene dendrons and shows an energy "cascade" from the dendrons to a lone perylene chromophore at the focal point.[20] Frechet has developed the approach of using laser-dye functionalized dendrimers incorporating highly fluorescent, soluble chromophores into a well-defined macromolecular array.[6] Nearly quantitative through-space energy transfer from the dendrimer periphery to its core was demonstrated by this approach with an appropriate choice of chromophores. From these studies, and others, it appears that an important issue in the efficient energy transfer in organic dendrimer architectures in the role of delocalized excited

[a)]Electronic mail: tgoodson@chem.wayne.edu

states in the transfer of excitation energy from the dendrons to the core.

Several mechanisms of excitation energy transfer can be considered in case of the relatively closely packed dendrimer system such as Coulombic dipole–dipole interactions,[23] short-range orbital-overlap interactions,[24,25] and superexchange coupling.[26] High fluorescence quantum efficiencies and molar extinction coefficients, as well as good overlap between donor emission and acceptor absorption support a proposed Coulombic mechanism of energy transfer in several reported organic dendrimer systems.[6,10,20] In many cases, it may be feasible to utilize the Coulombic theory in its simplest form such as the Förster theory alone. There have also been reports of more detailed calculations of the linear optical properties in dendrimer architectures. Mukamel *et al.*[11] has utilized the collective electronic oscillator method to construct an effective Frenkel exciton Hamiltonian for conjugated dendrimers with fractal geometry. For the phenylacetylene dendrimer system it was found that the linear optical response was dominated by localized excitons belonging to the periphery. The calculations showed that the molecule might be viewed as a weakly interacting ensemble of nearest neighbor, two-level chromophores.[11,12]

The excitation energy transfer rates in dendrimers (from dendrons to the core) may be estimated using either (or both as in this report) steady-state and time-resolved fluorescence data. Kopelman *et al.*[22,27] has demonstrated the correlation between the molecular geometry and the electronic properties utilizing a phenylacetylene dendrimer system. The results of steady state measurements for this system showed that the energy transfer efficiency increased with the generation number. It was also found that excitation transfer to the core decreased for generations higher than the sixth. Fleming *et al.*[6] have utilized both methods to obtain energy transfer rates for the laser-dye system mentioned above.[6] The steady-state method may have several difficulties due to the corrections needed for the excitation spectra. The very large efficiencies reported could be prone to moderate levels of error for this reason, and this method may not be used alone for the calculation of the energy transfer rate. Moore *et al.* has calculated the energy transfer rates using both steady-state spectra and time-resolved fluorescence.[20] The singlet–singlet energy transfer efficiency for one of the dendrimer systems was found to be 54% when the corrections for the excitation spectra where taken into account. In Moore's system it was also seen that the energy transfer efficiency decreased with increased generation. This was explained in the context of the Förster energy transfer theory.

There have been several reports that have not only investigated the energy transfer parameters, but also the nature of intermolecular interaction in dendrimer structures. DeSchryver *et al.* has studied a multichromophore dendrimer system which suggest the occurrence of intermolecular interactions among the chromophores within the dendritic structure.[28] There results also suggested the presence of excimerlike intermolecular quenching and aggregation. Meijer *et al.* has investigated a novel multiporphyrin dendrimer system in a glass environment using time-resolved fluorescence spectroscopy.[29] Time-resolved fluorescence anisotropy measurements were performed for a range of porphyrin dendrimer system of different spherical sizes. While the first generation system, again, agreed well with the Förster-type energy transfer between all porphyrin chromophores in the dendrimer, the result with a higher generation dendrimer suggested that the energy transfer was confined to only the porphyrins contained in one dendron.[29] The use of fluorescence anisotropy has also been shown to be instrumental in locating the position of energy transfer in dendrimer solutions. The time scale of this depolarization can be correlated with the excitation energy redistribution rate between the branches as this process is accompanied by the reorientation of the transition dipole moment. The fluorescence anisotropy dynamics combined with the isotropic time resolved and steady state spectroscopy may yield information about the interchromophore energy transfer character.[30–34] For example, there is a possibility of energy hopping from one donor to another along the dendrimer periphery. This may be inferred as an incoherent process and it will have a particular time constant and "hopping" distance that may be reflected in the depolarization rate.[32] Also, for delocalized excited states the energy transfer may be inferred as a coherent process and will have its own particular parameters that can be related to the depolarization rate.[30,31,33] Finally, for the case of no energy migration (or intermolecular interaction) the depolarization rate should follow the rotational diffusion of the dendrimer molecule in solution, which is relatively long for large molecules.[35]

Similar to the approach often taken in describing the dynamics of photosynthetic systems, the coherence of excitation in dendrimers can be analyzed by the two limiting cases of Förster transfer and that of completely delocalized excitonic states. The bridge between the two limiting cases is a parameter that describes the interaction energy (J) divided by the homogeneous linewidth Γ. If dipole–dipole nearest neighbor interactions are considered the molecular system can be described by the interacting Hamiltonian given by

$$H_T = H_0 + H_i + V_{\text{ex-ph}} + H_{\text{ph}},$$
$$H_0 + H_i = \sum_i \hbar\omega_i |i\rangle\langle i| + \frac{1}{2}\sum_{i\neq j} J_{ij}(|i\rangle\langle j| + |j\rangle\langle i|), \tag{1}$$

where $|i\rangle$ and $|j\rangle$ denote electronic states in which molecule i (or j) is excited. The first term in Eq. (1) corresponds to the transition energies of the molecules. The second term is the interaction term, where interactions can be transferred from molecule i to another molecule j. The third term is the exciton–phonon interaction term. The last term is the photon Hamiltonian. Leegwater[31] has considered the extent of delocalization theoretically by utilizing a Green's function approach as a function of electronic coupling and the homogeneous linewidth. This formalism is approximated in the high temperature limit, which is associated with an extremely short phonon correlation time. In spite of the last limitation (high temperature) the analytical results can be used for a qualitative description of the energy migration process. While this model contains interesting aspects of coherence in aggregated systems, its relationship to the fluorescence depo-

larization time and interaction parameter is the focus of our use in this study. It has been found that the depolarization time t_{dep} can be described by[31]

$$t_{\mathrm{dep}}=\frac{1}{\Gamma}\frac{1}{(1-G_0T)}, \tag{2}$$

where

$$G_0T=\frac{1}{N}\sum_{k=1}^{N}\frac{\Gamma^2}{\Gamma^2+16J^2\sin^2(2\pi/N)\sin^2(2\pi k/N)}.$$

In this equation J is the nearest neighbor interaction, Γ is the homogeneous linewidth, N is the number of chromophores, and G_0T is the product of noninteracting Green function and T matrix.[31] This relatively simple model does not take into account inhomogeneous broadening.[31] At the same time for small dendrimer molecules, which have been synthesized using very defined synthesis routes,[18] we do not expect a large static chromophore disorder such as that for pigments in natural light harvesting photosynthetic systems.[13–15] And here, we will use this analytical model to describe qualitatively the fast depolarization of emission in organic dendrimers.

In this paper the photophysics of the A-DSB stilbene dendrimer system is reported. The steady-state absorption, emission, and excitation spectra are given to estimate the energy transfer efficiency in the dendrimer systems. The A-DSB systems were originally synthesized for light emitting diode applications,[3–5] and the detailed measurements of their electroluminescence efficiencies have already been reported.[5] The femtosecond isotropic decay of the fluorescence at different wavelengths is provided and is also used to estimate the energy transfer rate. The fluorescence decay profile is given for the aldehyde dendrons, which are used as model compounds. The ultrafast fluorescence anisotropy decay for the different generations of dendrimers is provided. The model compound bis-MSB, which is related to the A-DSB core structure is also investigated for a comparison. These measurements are motivated by the quest for further understanding of the mechanisms involved in energy transfer processes in dendrimers, the role of delocalization, and the effect of intermolecular interactions in dendrimer structures.

II. EXPERIMENT

The dendrimers and dendron used in this study are shown in Fig. 1. The core of the dendrimers consists of a central nitrogen atom, to which three distyrylbenzene (DSB) units are connected. G2 dendrons, consisting of *meta*-linked stilbene units, are attached to this core, and *t*-butyl surface groups confer solubility in a range of organic solvents. The dendrimers G0, G2 materials can be readily spin-coated to form good quality films, and have been successfully used to make organic light-emitting diodes.[5] The degree of branching (generation number) determines the size of the molecule and provides an innovative way of controlling the charge mobility in films.[5] In this paper, we focus on the properties of the isolated molecules in solution and in particular the zero (G0) and second generation dendrimers (G2) together with the second generation aldehyde dendrons (SD2). This

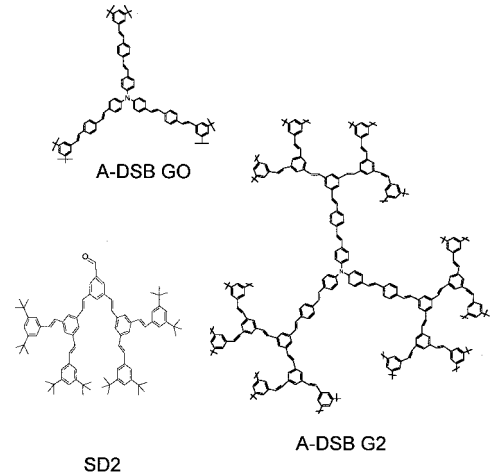

FIG. 1. The structure of aldehyde dendrons SD2. A-DSB dendrimers of zero (G0) and second (G2) generations.

selection of materials therefore allows the properties of the core, dendron, and dendrimer to be studied in a systematic manner.

UV-visible absorption spectra were recorded with a Hewlett-Packard 8452A diode array spectrophotometer and the fluorescence spectra were measured with a Shimadzu RF-1501 spectrofluorophotometer. Photoluminescence excitation spectra were measured using an Instruments SA Fluoromax fluorimeter. Time-resolved polarized fluorescence was studied by using the femtosecond up-conversion spectroscopy technique. The upconversion system used in our experiments is described in detail elsewhere.[36–38] Briefly, the sample solution was excited with a frequency-doubled light from a mode-locked Ti-sapphire laser (Tsunami, Spectra Physics). This produces pulses of approximately 100 fs duration in a wavelength range of 385–430 nm. The polarization of the excitation beam for the anisotropy measurements was controlled with a Berek compensator. The sample cuvette was 1 mm thick and is held in a rotating holder to avoid possible photodegradation and other accumulative effects. The horizontally polarized fluorescence emitted from the sample was up-converted in a nonlinear crystal of β-barium borate using a pump beam at about 800 nm that was first passed through a variable delay line. This system acts as an optical gate and enables the fluorescence to be resolved temporally with a time resolution of about 200 fs (pump-excitation 790/395 nm cross correlation function had a FWHM of 190 fs). Spectral resolution was achieved by dispersing the up-converted light in a monochromator and detecting it by using a photomultiplier tube (Hamamatsu R1527P). The excitation average power was kept at this level of below 0.5 milliwatts. In this excitation intensity regime the fluorescence dynamics was found to be independent of the excitation intensity for all investigated solutions.

This up-conversion technique is excellent in providing time-dependent fluorescence data on the femtosecond and picosecond time scales. Measurements on the ns time scale were also carried out by time-correlated single photon counting following excitation using an IBH nanosecond flashlamp. In both femtosecond and nanosecond measurements fluores-

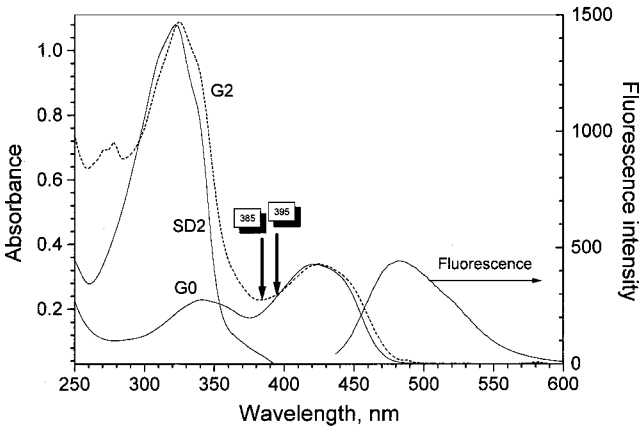

FIG. 2. Absorption spectra of dendrimers G0, G2 in chloroform solution normalized to the absorption of A-DSB core. Fluorescence spectrum of G2 under excitation at 420 nm is also shown. Absorption spectra of aldehyde stilbene dendrons of the second generation (SD2) in chloroform solution.

cence decay curves were fitted to the result of the convolution of the instrument response function with an exponential model to minimize the reduced χ^2 value.[39] The minimum value was obtained by the Marquardt nonlinear least squares method. The quality of the fit was monitored by values of the reduced χ^2 as well as by inspection of the residuals and autocorrelation function.

III. RESULTS

A. Steady state absorption and emission spectra

The absorption spectra of the G0 and G2 dendrimers together with the SD2 dendron in chloroform are shown in Fig. 2. The G2 dendrimer spectrum resembles a superposition of the absorptions due to the core and to stilbene. This might be expected because of the *meta*-arrangement of the dendron link (cross conjugation). However, the spectra are not exactly a superposition: the absorption maximum of G2 at 320 nm associated with the stilbene groups in the dendrons is ~20 nm (2083 cm^{-1}, 0.25 eV) to the red of the peak observed for the stilbene in the same solvent. It has been suggested[4] that in spite of *meta*-linking stilbene, there is a small amount of π-electron delocalization in the dendrons. The absorption spectrum of aldehyde dendrons of the second generation system (SD2, shown in Fig. 2) showed the same absorption maximum as that obtained for the amino core dendrimer G2, which is also again redshifted relative to the absorption peak of the stilbene molecule. This suggests the assignment of the absorption band of G2 at 320 nm to the absorption of dendrons in the dendrimer molecule. The redshift relative to the stilbene absorption peak could be an indication of some degree of exciton delocalization beyond one stilbene unit in the stilbene dendrons dendrimer shell. The absorption maximum in G2 dendrimer associated with the core is very slightly shifted to the red from the A-DSB absorption spectrum in G0.

The fluorescence spectra of G0 and G2 in chloroform were found to be similar and independent of excitation wavelength. The result for G2 is presented in Fig. 2 and shows that the emission is entirely from the core of the dendrimer.

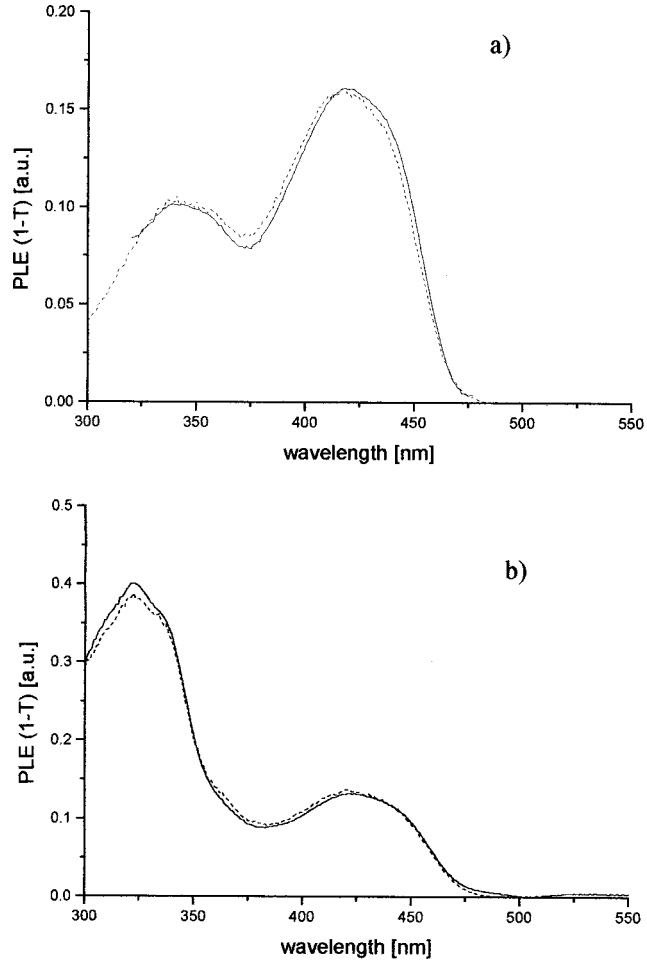

FIG. 3. (a) Optical spectra for G0 dendrimer. Solid line is absorption spectrum and dashed line is photoluminescence excitation (PLE) spectrum, (b) absorption and PLE spectra for G2 dendrimer.

Even when this molecule is excited at the peak of the dendron absorption, no steady state dendron emission is observed. This suggests that energy transfer from the dendron to the core is very efficient. We have investigated this further using photoluminescence excitation (PLE) spectroscopy. In a sample in which the photoluminescence quantum yield is independent of excitation wavelength, the intensity of luminescence will be proportional to the number of photons absorbed. The PLE spectra of G0 and G2 are shown in Fig. 3. A plot of $(1-T)$ where T is the transmission of the sample is shown for comparison. $(1-T)$ is a measure of the absorption of the sample and proportional to the number of photons absorbed. The fact that the absorption and PLE spectra are coincident across the entire excitation spectrum indicates that the efficiency of energy transfer from the dendron to the core is close to 100%.

B. Time-resolved isotropic fluorescence measurements

To estimate the influence of intramolecular stilbene dendron-core interaction in dendrimers of high generations to their fluorescence dynamics the time-resolved fluorescence of the model systems G0 (core) and aldehyde dendrons (SD2) (outer shell) was initially studied. Ultrafast fluores-

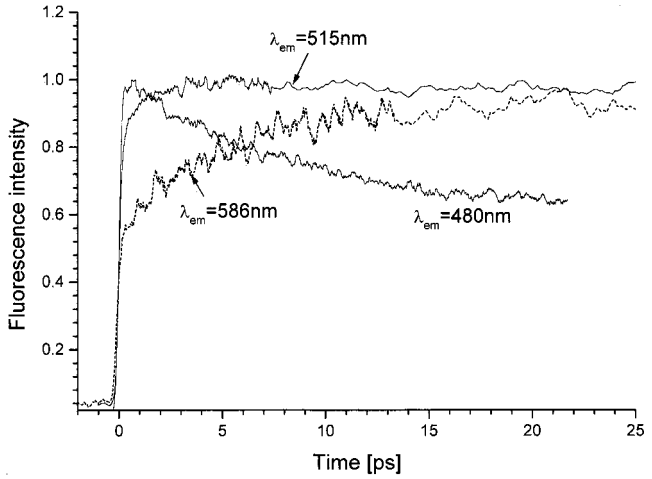

FIG. 4. Fluorescence decay of G0 at different emission wavelengths. Excitation wavelength was of 395 nm.

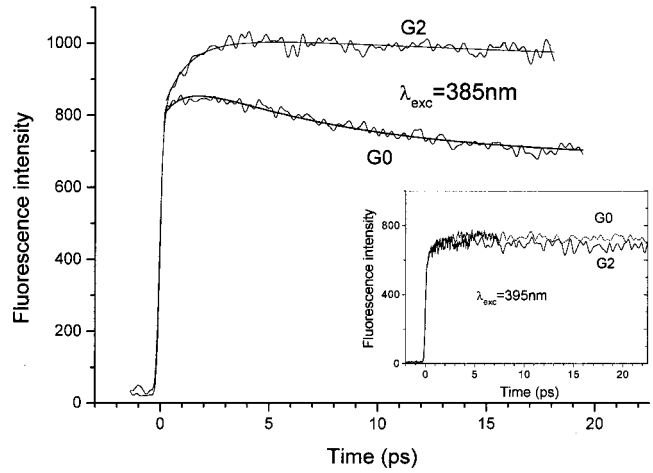

FIG. 6. Comparison of fluorescence decay of G0 with that of G2 at 515 nm. Excitation wavelength was of 385 nm. Inset: the same at excitation wavelength 395 nm.

cence dynamics of the core showed the dependence of the fast fluorescence dynamics pattern with emission wavelength (Fig. 4). A fluorescence risetime is observed at longer wavelengths. Generally, these dynamics could be associated with either solvent rearrangement or photoinduced solute conformational changes.[40,41] The aldehyde dendron (SD2) can be helpful for distinguishing between these possibilities. It was measured on the same time scale and in the same solvent as the dendrimer, but as can be seen in Fig. 5 (inset), does not show fast rise or decay features. We therefore propose conformational changes[42] of the excited dendrimer core to be the origin of the fluorescence dynamics of G0 shown in Fig. 4.

Nanosecond time-resolved luminescence measurements were carried out at a range of excitation and detection wavelengths for G0 and G2, and the decays were close to monoexponential with a time constant of 1.8 ± 0.2 ns. This value is typical of a strongly absorbing organic molecule. The lifetime of the dendron SD2 was measured to be 1.3 ± 0.2 ns. The fluorescence dynamics of SD2 on subnanosecond time scale is shown in Fig. 5. It can be described by a two-exponential decay law with time constants 116 ps and 1.3 ns.

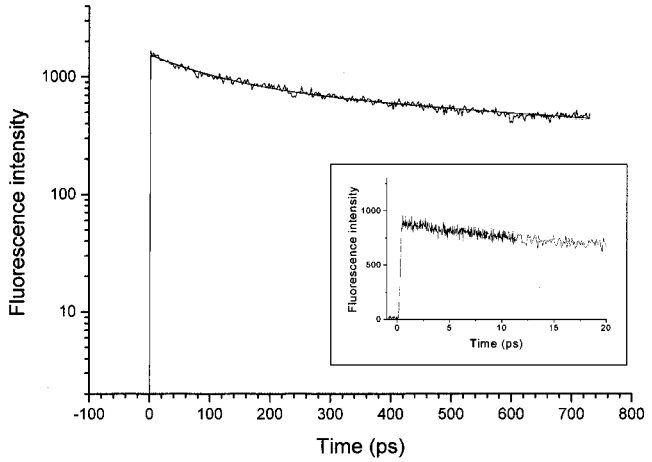

FIG. 5. Fluorescence decay of aldehyde dendrons SD2 at emission wavelength 480 nm. Excitation wavelength was of 385 nm. Inset: short time-scale decay.

The slowly decaying component is in good agreement with that obtained with nanosecond time-resolved luminescence measurements. It is established that the fluorescence lifetime of *trans*-stilbene in solution is of the order of 70 ps (depending on the solvent) and directed by a *trans cis* photoisomerization process.[43] The appearance of a long-lived component in the stilbene dendrons results as compared to the isolated *trans*-stilbene may indicate the delocalization of excitation beyond one stilbene unit in the stilbene dendron. Such a possibility was suggested above on the basis of steady state spectral measurements. Delocalization of the excitation could contribute to a significant hindrance to photoisomerization (conformation) processes thus leading to elongation of the fluorescence decay time.[37,42,44]

To probe the intramolecular interaction between stilbene dendrons shell and A-DSB core we compared the fluorescence kinetics for the dendrimer with and without stilbene dendrons: G0, G2. Chloroform solutions with concentrations $\sim5\times10^{-5}$ M were used in this experiment. The result is shown in Fig. 6. The decay curves in the figure (and also the inset) have been normalized in accordance with the peak absorption of the dendrimer cores of G0 and G2 at 420 nm. It is clearly seen from Fig. 6 that the fluorescence dynamics of G2 differ from those of G0 when fluorescence is excited at 385 nm. However, under excitation at 395 nm fluorescence decay curves for G2 and G0 are almost identical (Fig. 6, inset). Arrows in the absorption spectrum (shown in Fig. 2) label both excitation wavelengths 385 and 395 nm. It is clearly seen in Fig. 2 that additional absorption appears in G2 as compared to G0 when excitation is shifted from 395 nm to 385 nm. As the absorption peak of G2 at 320 nm is associated with the absorption of stilbene dendrons an appreciable part of the incident light was absorbed by stilbene dendrons of the G2 in case of excitation at 385 nm. The energy absorbed by stilbene dendrons at 385 nm could be transferred to the core. Therefore there are two channels for the excitation of the G2 core at 385 nm: direct excitation and the excitation via energy transfer from the dendrons. Thus we can attribute the difference between fluorescence dynam-

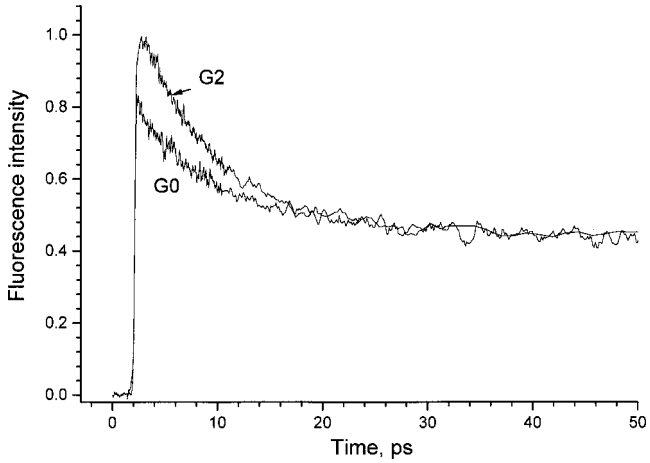

FIG. 7. Comparison of fluorescence decay of G0 with that of G2 at 480 nm. Excitation wavelength was of 385 nm. Fluorescence signals are normalized at the delay position of 40 ps.

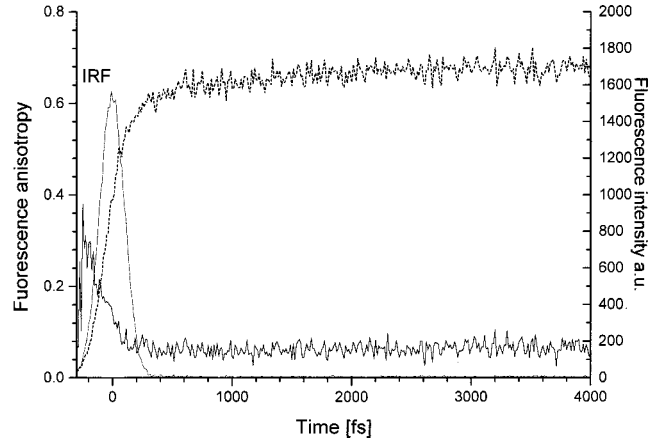

FIG. 8. Fluorescence anisotropy decay for G2 at 515 nm. The isotropic fluorescence dynamics and the instrument response function profile are also shown. The excitation wavelength was 385 nm.

ics of G2 and G0 at the excitation wavelength 385 nm to the energy transfer from dendrons to the core in case of G2.

We have also measured the fluorescence dynamics of G2 and G0 at shorter emission wavelengths 480, 450 nm. The results for $\lambda_{em}=480$ nm is shown in Fig. 7. An additional fast component is clearly seen for G2 as compared to that for G0. We also found the relative contribution of the short-lived component of G2 relative to that for G0 to increase with the emission wavelength decrease from 480 to 450 nm. The fluorescence spectrum of aldehyde dendrons (model system for donor) had a maximum at about 415 nm (shown in Fig. 2). The additional fast component in the fluorescence dynamics of G2 with respect to the G0 dynamics at relatively short emission wavelengths can be tentatively attributed to the fluorescence of the dendron before energy transfer to the core takes place.

C. Fluorescence anisotropy decay measurements

To gain a further insight into energy transfer (energy migration) processes in A-DSB dendrimer molecules we investigated the fluorescence anisotropy dynamics in G0 and G2. Preliminary results on the fluorescence anisotropy in G0 and G2 have been reported in our previous short communication.[45] Experimental florescence anisotropy $R(t)$ was calculated from the decay curves for the intensities of fluorescence polarized parallel $I_{\mathrm{par}}(t)$ and perpendicularly $I_{\mathrm{per}}(t)$ to the polarization of the excitation light according to the equation

$$R(t)=\frac{I_{\mathrm{par}}-GI_{\mathrm{per}}}{I_{\mathrm{par}}+2GI_{\mathrm{per}}}. \tag{3}$$

The factor G accounts for the difference in sensitivities for the detection of emission in the perpendicular and parallel polarized configurations. This factor was measured using perylene in methanol as a reference. In the real experiment the G factor has been found to be essentially unity (1.02 $\pm$0.02). The results of depolarization measurements in G0 and G2 are shown in Figs. 8 and 9. The fluorescence anisotropy decays to a small residual value of about 0.06 within the instrument response function duration and remains unchanged during the fluorescence decay time. Fluorescence anisotropy profiles are seen to be very similar for G0 and G2 indicating the fast fluorescence depolarization process is predominantly associated with the dendrimer core and not sensitive to presence of the stilbene dendrons. It is also worth noting that $R(t)$ for G0 was found to be independent of the excitation wavelength in the range 385–430 nm. The last observation is very important with regard to the possible explanation of low fluorescence anisotropy. For example, it can be suggested that low value of fluorescence anisotropy is associated with simultaneous excitation of two different electronic transitions with mutually different orientations of dipoles followed by the emission from one of them possessing lower energy (relaxed state). In this situation it is possible to find the excitation wavelength at which the emission will be completely depolarized as it takes place for simultaneous excitation of S_2 and S_1 transitions in simple molecules.[46] Obviously this is not the case for A-DSB as no appreciable excitation wavelength dependence of the residual anisotropy was observed.

To gain a further insight into the physics behind the fast depolarization process we measured the fluorescence anisot-

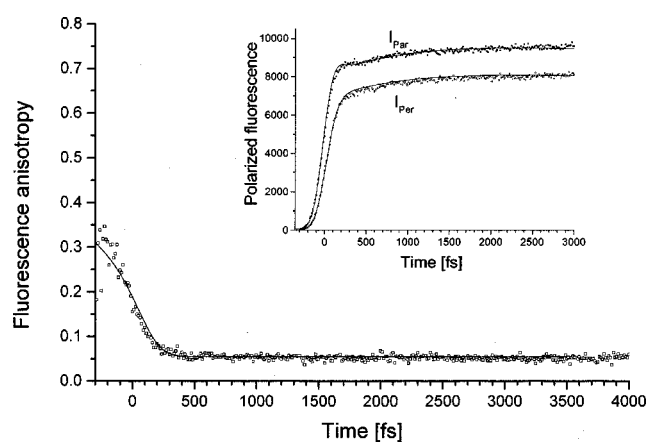

FIG. 9. Fluorescence anisotropy decay for G0 at 515 nm. Excitation wavelength was of 410 nm. Best fit curves are also shown (see the text).

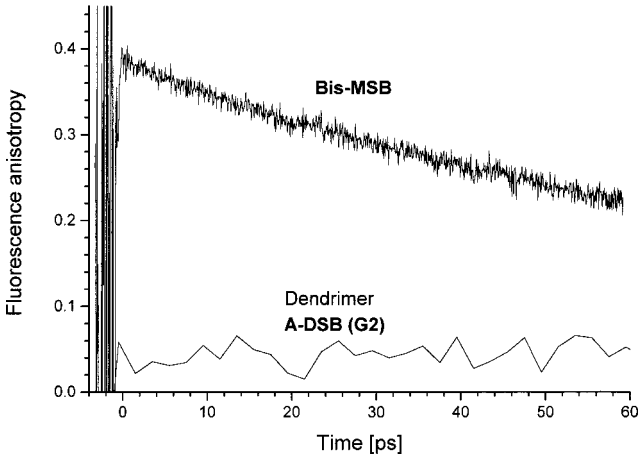

FIG. 10. Fluorescence anisotropy decay for the model system bis-MSB. Anisotropy dynamics of G2 is shown for comparison.

ropy for the model system of *p*-bis(o-methylstyryl)–benzene (bis-MSB) representing the linear building block of the G0. The result is shown in Fig. 10. It is clearly seen that fluorescence anisotropy dynamics of the model system of bis-MSB strongly differs from that of dendrimer. Starting at the initial value close to 0.4 fluorescence anisotropy decays with the time constant of 82 ps, which agrees with the rotational diffusion time of bis-MSB molecule. For G0 and G2 it was difficult to see the contribution of overall molecular rotation as the fluorescence anisotropy dropped to a very small residual value within the time interval of ~200 fs, which is much shorter than any reasonable time scale of rotational movement. Comparing the anisotropy decay results for G0 and G2 with those for the model system bis-MSB suggests ultrafast transition dipole reorientation due to intersegment interactions in these dendrimers.

IV. DISCUSSION

A. Energy transfer from stilbene dendrons to A-DSB core

The PLE results suggest that the efficiency of energy transfer from the dendron to the core of G2 is close to 100%. This result is consistent with PLE measurements on related dendrimers based on DSB (no nitrogen), DSB anthracene, and porphyrin[4,18] in which energy transfer was found to take place with efficiency approaching unity.[18] The time-resolved measurements also provide a means of estimating the efficiency of energy transfer. The first step is to estimate the rate of energy transfer from dendron to core. To do this we fit the decay curve for G0 using two exponential decay functions with the pre-exponential factors A_1, A_2 and residual (long-lived) fluorescence A_r:

$$Y_o(t) = A_1 \exp\left(\frac{-t}{\tau_1}\right) + A_2 \exp\left(\frac{-t}{\tau_2}\right) + \theta(t)*A_r. \tag{4}$$

Here τ_1, τ_2 are decay times and $\theta(t)$ is a step function. Then we fit the decay curve for G2 using three exponential decay functions with pre-exponential factors B_1, B_2, B_3 and residual long-lived fluorescence B_r:

$$Y_0(t) = B_1 \exp\left(\frac{-t}{\tau_1}\right) + B_2 \exp\left(\frac{-t}{\tau_2}\right) + B_3 \exp\left(\frac{-t}{\tau_3}\right) + \theta(t)*B_r. \tag{5}$$

In the last fit we kept the decay times τ_1, τ_2 fixed and equal to those obtained for G0. As a result of this procedure we found B_3 to be negative (corresponding to additional risetime component) and τ_3 equal to 7.2 ± 1.0 ps. This observed additional risetime in the fluorescence dynamics of G2 determines the energy transfer rate constant $k_{ET} \cong 1/\tau_3$. It is worth noting that additional fast component observed in the emission of G2 at 480 nm, which has been assigned to emission of stilbene dendrons (see Fig. 7 and related text), possesses about the same decay time constant as the risetime at 515 nm. This indicates the decay of donor (dendrons) to be essentially controlled by the energy transfer process to the acceptor (A-DSB core).

To estimate the relative contribution of the core fluorescence excited via energy transfer from dendrons relative to that of directly excited core we performed the model calculations of the fluorescence dynamics in case of simultaneous excitation of a donor and acceptor. For these model calculations we suggested the donor excited state decay to be completely directed by the energy transfer process. We also assumed the acceptor decay under direct excitation to be two exponential with the second time constant to be very long (residual long-lived fluorescence). This decay function contains one fast exponential instead of two used in the best fit of a real acceptor [Eq. (4)]. With these simplifications it is possible to derive the analytical expression for the time-dependent fluorescence intensity using the procedure analogous to that for excimer emission.[47] The relative contribution of directly excited acceptors was estimated using the best fit data to experimental decays to be 0.81. This is in reasonable agreement with the rough estimation of this ratio from the comparison of the fluorescence intensities (see Fig. 6 and normalization procedure described above), which has been found to be 0.73.

In a weak coupling limit of Eq. (1), when the homogeneous linewidth is much larger than the interchromophore interaction the energy transfer can be described as a hopping of excitation. This case is referred to as the Förster limit.[23] To evaluate the ability of the theory[23] to describe the energy transfer from dendrons to the core in G2, we compare the theoretical and measured energy transfer rates. The Förster's rate of energy transfer between donor and acceptor separated by a distance R_{DA} is given by

$$k_t(r) = \frac{1}{\tau_D}\left(\frac{R_F}{R_{DA}}\right)^6, \tag{6}$$

where τ_D is the fluorescence lifetime of the donor in the absence of acceptor and R_F is the Förster radius, which is the critical distance between the donor and acceptor such that the energy transfer probability equals the emission probability. R_F can be calculated using the following equation:[23]

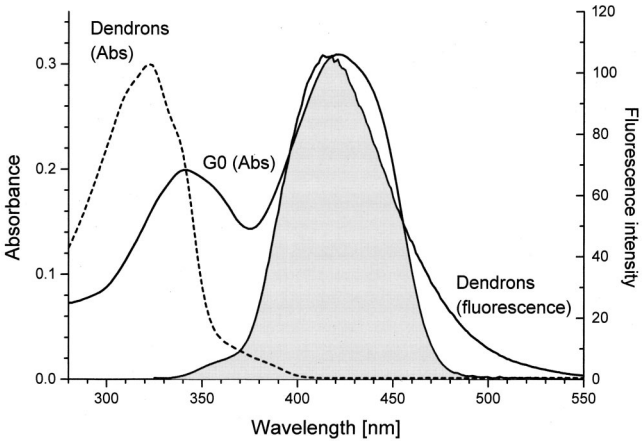

FIG. 11. The spectral overlap of the aldehyde dendrons (donor) fluorescence and G0 (acceptor) absorption.

$$R_F^6 = \frac{9000(\ln 10) Q_D \kappa^2 J}{128 \pi^5 N_A n^4}, \tag{7}$$

where Q_D is the fluorescence quantum yield of the donor, N_A is Avogadro's number, n is the refractive index, k^2 is the orientation factor, and J is the spectral overlap integral of the emission of donor with the absorption of acceptor. The overlap integral $J(\mathrm{M}^{-1}\,\mathrm{cm}^3)$ is given by

$$J = \int_0^\infty F_D(\lambda) \cdot \epsilon_A(\lambda) \cdot \lambda^4 \cdot d\lambda, \tag{8}$$

where $\epsilon_A(\lambda)$ is the molar extinction coefficient of the acceptor and $F_D(\lambda)$ is the emission spectrum of the donor normalized according to $\int F_A(\lambda) d\lambda = 1$. In our calculations k^2 is given a value of 2/3, which corresponds to the averaging of all possible mutual orientations during energy transfer time. This is a reasonable assumption as the depolarization rate of the acceptor (G0) is extremely high in our case (see Figs. 8 and 9). The fluorescence quantum yield of SD2 is not accurately known but it can be roughly estimated to be 0.3 using bis-MSB as a reference. Bis-MSB absorption and fluorescence spectra are similar to those for aldehyde dendrons and its quantum yield is close to unity.[48] The fluorescence spectrum of aldehyde dendrons (donor) and the spectral overlap with absorption spectrum of G0 (acceptor) is shown in Fig. 11. From this figure it is clearly seen that the overlap of the donor emission and the acceptor absorption is excellent indicating that probability of donor–acceptor energy transfer should be high. Indeed, the Förster radius R_F calculated in accordance with Eq. (7) was equal to 46 Å. To calculate the theoretical energy transfer rate k_t it is necessary to estimate the interchromophore distance R_{DA}. Assuming $R_{DA} = 17$ Å (the distance between center of the core nitrogen and the nearest double bond of a stilbene dendron) an energy transfer rate of $k_t = 0.3 \times 10^{12}\ \mathrm{s}^{-1}$ is obtained. This transfer rate corresponds to transfer time of 3.3 ps. This is about two times faster than the energy transfer time estimated from time-resolved measurements. However, one should take into account that only the homogeneous line shape should be used for evaluating the overlap integral.[23] Using observed absorption and emission lines in the calculation of the overlap integral can lead to an overestimate of the excitation transfer rate. Additionally, the very rough estimation of the yield of SD2 could also lead to a discrepancy between calculated and experimental transfer rate. It is worth noting that there is no obvious necessity to use other than the Förster mechanism to describe the energy transfer in the case of A-DSB dendrimer.

The energy transfer efficiency can be estimated using the following relationship:

$$\Phi_{\mathrm{ET}} = \frac{k_t \tau_D}{1 + k_t \tau_D}. \tag{9}$$

Taking τ_D to be equal to the measured value of the dendron lifetime of 1.3 ns, and $1/k_t$ equal to 7.2 ps gives a value of Φ_{ET} of 99.5%, confirming the high efficiency of energy transfer deduced from steady state measurements.

B. Interaction between DSB branches

It should be noted that the zero-generation unit G0 (actually the dendrimer core) is not a simple DSB segment. It is a starlike molecule consisting of three DSB segments bonded to a central nitrogen atom. The absorption of the G0 is shifted to the red by 3969 cm^{-1} (0.49 eV) as compared to that for DSB. It can be suggested that this shift is due to either mesomeric effect from the electron rich nitrogen core atom and/or due to some delocalization between the DSB units allowed by nitrogen.[5] The dipole–dipole interaction between DSB units is also possible. These different interactions could lead to the formation of coherent excitonic states[31,49,50] or hopping-type relaxation of excitations completely localized on one DSB branch (incoherent interaction[51,52]).

It may be suggested that the residual fluorescence anisotropy of G0 is nearly zero because of an irreversible relaxation to a state with the transition dipole orientated at about 55° (magic angle) with respect to the initially excited one. However, this simple two-state model is not reasonably applicable to our particular symmetrical geometry. For example, in the A-DSB system a more realistic angle of 60° (120°) and for the case of one irreversible step the fluorescence anisotropy should be negative (−0.05). However, our results show a positive value close to what is expected for the equilibrium process in a symmetrical molecule with three branches.

Exciton migration via intramolecular excitation transfer in molecules or molecular complexes with high degree of symmetry was experimentally investigated in a number of publications.[51,53–56] Using fluorescence depolarization it is possible to observe this intramolecular excitation transfer because the latter process is accompanied by the reorientation of the transition dipole resulting in depolarization of the emission. Fast decay of fluorescence anisotropy (few picoseconds) in an amino-substituted triphenylbenzene derivative, (*p*-EFTP), was detected by femtosecond polarized transient absorption.[51] The fast depolarization was assigned to an exciton migration (hopping, incoherent interaction) between the branches of this threefold symmetry molecule.[51] The excitation dynamics in several threefold and fourfold symmetry branched molecules was probed by the time-resolved fluorescence anisotropy.[56] Both Förster-type incoherent energy

migration between branches and excitonic-type coherent transport mechanism could be observed depending on molecular architecture.[56] A general description of fast depolarization in a symmetrical branched molecular system is the relaxation of a superposition of degenerate states with different orientations of transition dipoles. An analysis of the fluorescence anisotropy associated with twofold and threefold degenerate states with different orientation of transition dipoles has been discussed by Wynne and Hochstrasser.[30] The case of excitonic splitting for dimers,[30,49] the role of nuclear degrees of freedom (vibrations),[50,55] as well as depolarization in higher molecular aggregates with static disorder[57] were also analyzed. It is a remarkable feature of symmetrical molecular systems that they can exhibit an initial anisotropy larger than 0.4, the initial anisotropy observed in a collection of randomly oriented single chromophores.[30,49] The second important parameter is the residual anisotropy for the equilibrated system. This parameter is also strongly related to the geometry of the molecular system and should be 0.1 for simple in-plane symmetrical dipoles arrangement[30,32,49–55] while in three-dimensional structures it can drop to zero[30] (in the absence of overall molecular rotation).

In G0 three distyrylbenzene chromophores are supposed to be grouped in a ''propeller''-like arrangement around the nitrogen.[58] The angle between transition dipoles of adjacent DSB chromophores can be estimated to be $\sim 120°$ provided these dipoles are directed along the direction of the bonds to the nitrogen.[58] It is easy to calculate the residual fluorescence anisotropy after relaxation between branches just using the law of additivity of anisotropies.[59] This yields a residual anisotropy value 0.1 in this case. It is different than the observed value of about 0.06 (see Figs. 9 and 10). The reason for this difference could lay in a deviation of the directions of DSB transition dipoles from the directions of DSB–nitrogen bonds in the plane of the principal axis of the molecule. Such deviations lead to a different value of residual anisotropy[60] (an inclination angle relative to the N–C plane of about 15.8° could lead to the residual anisotropy of 0.06 observed in our experiments). This result suggests the transition dipole arrangement in this molecule in solution to slightly deviate from planar geometry.

The initial dynamics of fluorescence anisotropy is very fast, completing within the duration of the instrument response function (Fig. 9). Thus, it is difficult to analyze the fluorescence anisotropy decay law and deduce the initial anisotropy at a good confidence level. Application of standard deconvolution procedures for difference and isotropic decays is complicated by relatively large background noise in the vicinity of IRF, which is associated to some extent with the presence of the risetime feature in the isotropic decay.[32] To make a reasonable estimation of the fluorescence anisotropy decay time we performed impulse reconvolution[61] assuming simple one-exponential decay law for anisotropy decay with time constant τ_a and the residual value of τ_r. The isotropic fluorescence decay function was constructed using best fit results described above. This analysis yielded the anisotropy decay time τ_a of 57 ± 7 ps and the residual anisotropy τ_r of 0.055 ± 0.003. An initial anisotropy r_0 best fit result was of 0.42 ± 0.05. The best fit curves obtained for parallel and perpendicularly polarized fluorescence components as well as for raw anisotropy are shown in Fig. 9. The initial anisotropy for a molecule having symmetry higher than C_2 can significantly exceed the value 0.4 associated with photoselection of an isolated dipole.[30,49,50] However, our detection wavelength was redshifted relative to excitation. This implies that we were probing predominantly relaxed states for which the initial coherent superposition of the dipoles could be substantially destroyed. It should also be noted that our estimation of r_0 has been made on the basis of an oversimplified model of monophasic (monoexponential) anisotropy decay and information about very initial anisotropy behavior could not be sufficiently accurate.

Fluorescence depolarization combined with isotropic fluorescence decay and spectroscopic information can be a sensitive probe for the nature of energy transfer (exciton or hopping dynamics).[31,32,34] An extremely fast depolarization rate could indicate strong interaction between branches in the core. For this reason the weak interaction limit (Förster limit), which was used for interpretation of energy transfer between dendrons and the core could not be applicable for interbranch energy migration. Our estimation of the Förster transfer time between DSB branches gave the value of about 4 ps. To describe qualitatively the interbranch energy migration process we used the analytical general expression for the anisotropy decay rate k_{dep} in a ring molecular system at high temperature derived in[31]

$$k_{\mathrm{dep}}=\Gamma\left(1+\frac{1}{N}\sum_{k=1}^{N}\frac{\Gamma^2}{\Gamma^2+16J^2\sin^2\left(\frac{2\pi}{N}\right)\sin^2\left(\frac{2\pi k}{N}\right)}\right), \tag{10}$$

where J is the nearest neighbor interaction, Γ is the homogeneous linewidth, N is the number of chromophores, and $k_{\mathrm{dep}}=1/\tau_r$ is the inverse depolarization time. An inhomogeneous broadening is neglected in the approach.[31] For the system with three chromophores the expression (10) becomes

$$k_{\mathrm{dep}}=\frac{6\Gamma}{(\Gamma^2/J^2+9)}. \tag{11}$$

The dependence of depolarization time $\tau_a=1/k_{\mathrm{dep}}$ on interchromophore interaction determined by Eq. (11) is shown in Fig. 12. For the region where the homogeneous linewidth is much larger than the interchromophore interaction ($\Gamma \gg J$), the energy transfer can be described as a hopping of excitations. The opposite limit ($\Gamma \ll J$) is the exciton limit where the system can be considered as molecular aggregate with its own excitonic energy levels.[31–34] It is seen from Fig. 12 that the dependence of the depolarization rate on the interaction behaves differently in these two regions. The experiment on selective excitation of the G0 fluorescence showed no dependence of the fluorescence spectra on the excitation wavelength. This is an indication of predominantly homogeneously broadened transition on the time scale of steady state spectral measurements. However, time-resolved experiments showed the dependence of the fluorescence dynamics on the emission wavelength in the picosecond time range (see Fig. 4). Our analysis of the decay curves showed

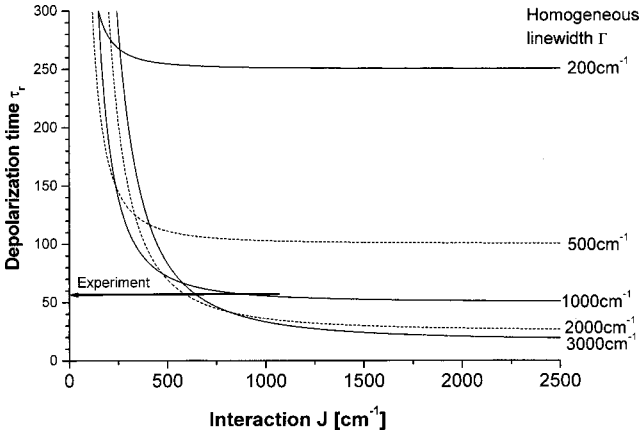

FIG. 12. The theoretical dependence of depolarization time τ_r on interchromophore interaction for C_3-three-chromophore molecular system. The depolarization time obtained from experimental is also shown by an arrow.

that the change in the fluorescence spectral width during the first several picoseconds after excitation is not substantial and we can suggest the linewidth on the picosecond time scale to be roughly the same as that on the time scale of steady state experiments. Additionally, we found no detectable dependence of the fluorescence dynamics on the excitation wavelength. These results allow us to suggest the homogeneous linewidth of G0 to be in the range of 1900–2900 cm^{-1}. The interaction J can be estimated using Eq. (11) to be about 600 cm^{-1} (it is also seen from Fig. 12). Figure 12 also shows that the energy transfer mechanism is consistent with the experimental depolarization rate (the experimental anisotropy decay time is marked off by an arrow), which is in the crossover region between hopping and excitation dynamics where the characteristics of exciton coherence cannot be ignored.

V. CONCLUSIONS

We have measured the photodynamics of a novel organic A-DSB dendrimer and estimated the energy transfer rate from the stilbene dendrons to the core. Steady state measurements showed the energy transfer efficiency to be approximately 99.5%, while time-resolved measurements showed the rate to be approximately 7 ps. Calculations of the energy transfer efficiency and rate from time resolved measurements agreed well with the steady state spectra, suggesting that at these lower generations the Förster model may be suitable in describing the mechanism of the energy transfer from dendrons to the core. The anisotropy decay of the A-DSB dendrimer system was very fast, decaying to a value of 0.055 in about 100 fs. The fast decay can be attributed to a coherent interchromophore energy transport in the core. The anisotropy results of model compounds related to the A-DSB dendrimer showed the reasonable result of long rotational diffusion decay and no energy transfer. This suggests that the core branched geometry facilitates the very fast anisotropy decay, and may play a large role in the intermolecular interaction in the similar dendrimer systems.

ACKNOWLEDGMENTS

The authors thank the Air Force Office of Scientific Research, The American Chemical Society–Petroleum Research Fund for partial funding of this project. I.D.W.S. is a Royal Society University Research Fellow. The authors thank Professor S. Mukamel for valuable discussions and M. Ranasinghe and J.P.J. Markham for assistance.

[1] D. A. Tomalia, H. Baker, J. R. Dewald, M. Hall, G. Kallos, S. Martin, J. Roeck, J. Ryder, and P. Smith, Polym. J. (Tokyo) **17**, 117 (1985).
[2] P. W. Wang, Y. J. Liu, C. Devadoss, P. Bharathi, and J. S. Moore, Adv. Mater. **8**, 237 (1996).
[3] J. M. Lupton, I. D. W. Samuel, R. Beavington, P. L. Burn, and H. Bässler, Adv. Mater. **13**, 258 (2001).
[4] M. Halim, I. D. W. Samuel, J. N. G. Pillow, and P. L. Burn, Synth. Met. **102**, 1113 (1999).
[5] J. M. Lupton, I. D. W. Samuel, R. Beavington, M. J. Frampton, P. L. Burn, and H. Bässler, Phys. Rev. B **63**, 155206 (2001).
[6] A. Andropov, S. Gilat, J. M. J. Frechet, K. Ohta, F. V. R. Neuvahl, and G. Fleming, J. Am. Chem. Soc. **127**, 1175 (2000).
[7] T. Goodson III, in *Dendrimers and Other Dendritic Polymers*, edited by J. M. J. Frechet and D. A. Tomalia (Wiley, New York, 2001), p. 515.
[8] A. Bar-Haim, J. Klafter, and R. Kopelman, J. Am. Chem. Soc. **119**, 6197 (1997).
[9] S. Raychaudhuri, Y. Shapir, V. Chernyak, and S. Mukamel, Phys. Rev. Lett. **85**, 282 (2000).
[10] A. W. Bosman, H. M. Janssen, and E. W. Meijer, Chem. Rev. **99**, 1665 (1999).
[11] S. Tretiak, V. Chernyak, and S. Mukamel, J. Chem. Phys. **110**, 8161 (1999).
[12] M. Nakano, M. Takahata, H. Fujita, S. Kiribayashi, and K. Yamaguchi, Chem. Phys. Lett. **323**, 249 (2000).
[13] V. Sundstrom, T. Pullerits, and R. van Grondelle, J. Phys. Chem. B **103**, 2327 (1999).
[14] H. van Amaerongen and R. van Grondelle, J. Phys. Chem. **105**, 604 (2001).
[15] R. van Grondelle and V. Novoderezhkin, Biochemistry **40**, 15057 (2001).
[16] X. J. Jordanides, G. Scholes, and G. R. Fleming, J. Phys. Chem. **105**, 1652 (2001).
[17] T.-Q. Nguyen, J. Wu, V. Doan, B. J. Schwartz, and S. H. Tolbert, Science **228**, 652 (2000).
[18] J. N. G. Pillow, M. Halim, J. M. Lupton, P. Burn, and I. D. W. Samuel, Macromolecules **32**, 5985 (1999).
[19] D. L. Jiang and T. Aida, J. Am. Chem. Soc. **120**, 10895 (1998).
[20] C. Devadoss, P. Bharrathi, and J. S. Moore, J. Am. Chem. Soc. **118**, 9635 (1996).
[21] T. Sato, D.-L. Jiang, and T. Aida, J. Am. Chem. Soc. **121**, 10658 (1999).
[22] R. Kopelman, M. Shortreed, Zhong-You Shi, W. Tang, Z. Xu, J. Moore, A. Bar-Haim, and J. Klafter, Phys. Rev. Lett. **78**, 1239 (1997).
[23] Th. Förster, Ann. Phys. (Leipzig) **2**, 55 (1948).
[24] D. L. Dexter, J. Chem. Phys. **21**, 836 (1953).
[25] D. D. Harcourt, G. D. Scholes, and K. P. Ghiggino, J. Chem. Phys. **101**, 10521 (1994).
[26] E. K. L. Yeow, D. J. Haines, K. P. Ghiggino, and M. P. Paddon-Row, J. Phys. Chem. A **103**, 6517 (1999).
[27] Y. S. F. Swallen, Z. Zhu, J. S. Moore, and R. Kopelman, J. Phys. Chem. **104**, 3988 (2000).
[28] Y. Karni, S. Jordens, G. DeBelder, G. Schweitzer, J. Hofkens, T. Gensch, M. Maus, F. C. DeSchryver, A. Herrmann, and K. Mullen, Chem. Phys. Lett. **310**, 73 (1999).
[29] E. K. L. Yeow, K. P. Ghiggino, J. N. H. Reek, M. J. Crossley, A. W. Bosman, A. P. H. J. Schenning, and E. W. Meijer, J. Phys. Chem. B **104**, 2596 (2000).
[30] K. Wynne and R. M. Hochstrasser, Chem. Phys. **171**, 179 (1993).
[31] J. A. Leegwater, J. Phys. Chem. **100**, 14403 (1996).
[32] S. E. Bradforth, R. Jimenez, F. van Mourik, R. van Grondelle, and G. R. Fleming, J. Phys. Chem. **99**, 16179 (1995).
[33] R. Kumble, S. Palese, R. W. Visschers, P. L. Dutton, and R. M. Hochstrasser, Chem. Phys. Lett. **261**, 396 (1996).
[34] S. Savikhin, D. R. Buck, and W. S. Struve, Biophys. J. **73**, 2090 (1997).
[35] H. Anderson, S. Anderson, T. Goodson III, and J. F. Ryan, J. Chem. Soc., Perkin Trans. 1 **7**, 2383 (1998).

[36] O. Varnavski, A. Leanov, L. Liu, J. Takacs, and T. Goodson III, J. Phys. Chem. **104**, 179 (2000).
[37] O. Varnavski and T. Goodson, Chem. Phys. Lett. **320**, 688 (2000).
[38] O. Varnavski, A. Leanov, L. Liu, J. Takacs, and T. Goodson III, Phys. Rev. B **61**, 12732 (2000).
[39] A. Grinvald and I. Steinberg, Anal. Biochem. **59**, 583 (1974).
[40] M. L. Horng, J. A. Gardecki, A. Papazyan, and M. Maroncelli, J. Phys. Chem. **99**, 17311 (1995).
[41] J.-F. Letard, R. Lapouyade, and W. Rettig, Chem. Phys. **186**, 119 (1994).
[42] C. M. Heller, I. H. Campbell, B. K. Laurich, D. L. Smith, D. D. C. Bradley, P. L. Burn, J. P. Ferraris, and K. Mullen, Phys. Rev. B **54**, 5516 (1996).
[43] S. H. Courtney and G. R. Fleming, J. Chem. Phys. **83**, 215 (1985).
[44] G. C. Bazan, W. J. Oldham, Jr., R. J. Lachicotte, S. Tretiak, V. Chernyak, and S. Mukamel, J. Am. Chem. Soc. **120**, 9188 (1998).
[45] O. Varnavski, G. Menkir, R. Beavington, I. D. W. Samuel, J. M. Lupton, P. L. Burn, and T. Goodson III, Appl. Phys. Lett. **77**, 1120 (2000).
[46] M. van Gurp, T. van Heijnsbergen, G. van Ginkel, and Y. K. Levine, J. Chem. Phys. **90**, 4103 (1988).
[47] J. B. Birks, Rep. Prog. Phys. **38**, 903 (1975).
[48] J. Sujatha and A. K. Mishra, J. Photochem. Photobiol., A **101**, 245 (1996).
[49] R. Knox and D. Gulen, Photochem. Photobiol. **57**, 40 (1993).
[50] A. Matro and J. A. Cina, J. Phys. Chem. **99**, 2568 (1995).
[51] L. Larettini, G. DeBelder, G. Schweitzer, M. Van der Auweraer, and F. C. DeSchryver, Chem. Phys. Lett. **295**, 11 (1998).
[52] I. V. Rubtsov, Y. Kobuke, H. Miyaji, and K. Yoshihara, Chem. Phys. Lett. **308**, 323 (1999).
[53] A. T. Yeh, C. V. Shank, and J. K. McCuster, Science **289**, 935 (2000).
[54] R. E. Riter, M. D. Edington, and W. F. Beck, J. Phys. Chem. B **101**, 2366 (1997).
[55] A. A. Ferro and D. M. Jonas, J. Chem. Phys. **115**, 6281 (2001).
[56] O. P. Varnavski, J. C. Ostrowski, L. Sukhomlinova, R. J. Twieg, G. C. Bazan, and T. Goodson III, J. Am. Chem. Soc. (in press).
[57] R. Kumble and R. M. Hochstrasser, J. Chem. Phys. **109**, 855 (1998).
[58] O. P. Varnavski, J. C. Ostrowski, L. Sukhomlinova, R. J. Twieg, G. C. Bazan, and T. Goodson III, J. Am. Chem. Soc. **124**, 1736 (2002).
[59] G. Weber, Biochem. J. **51**, 145 (1952).
[60] A. A. Demidov and D. L. Andrews, Photochem. Photobiol. **63**, 39 (1996).
[61] I. Soutar, L. Swanson, R. L. Christensen, R. Drake, and D. Phillips, Macromolecules **29**, 4931 (1996).